2011

Multiscale Modeling of Traffic Flow

Daiheng Ni, *University of Massachusetts - Amherst*

Mathematica Aeterna, Vol.1, 2011, no. 01, 27 - 54

Multiscale Modeling of Traffic Flow

Daiheng Ni

Department of Civil and Environmental Engineering
University of Massachusetts
Amherst, MA 01003, U.S.A
ni@ecs.umass.edu

Abstract

This paper presents a broad perspective on traffic flow modeling at a spectrum of four scales. Modeling objectives and model properties at each scale are discussed and existing efforts are reviewed. In order to ensure modeling consistency and provide a microscopic basis for macroscopic models, it is critical to address the coupling among models at different scales, i.e. how less detailed models are derived from more detailed models and, conversely, how more detailed models are aggregated to less detailed models. With this understanding, a consistent modeling approach is proposed based on field theory and modeling strategies at each of the four scales are discussed. In addition, a few special cases are formulated at both microscopic and macroscopic scales. Numerical and empirical results suggest that these special cases perform satisfactorily and aggregate to realistic macroscopic behavior. By ensuring model coupling and modeling consistency, the proposed approach is able to establish the theoretical foundation for traffic modeling and simulation at multiple scales seamlessly within a single system.

Mathematics Subject Classification: 03C98, 03C30, 03C99, 12E99

Keywords: Multiscale modeling, traffic flow, field theory.

1 Introduction

Anyone who used maps probably developed the following experience. Fifteen years ago, a 1:10,000 paper map was needed to view a city (e.g. Amherst, MA), while a 1:1,000,000 paper map was needed to view a state (e.g. Massachusetts). If the scale was changed, a new map was needed. Today, using digital maps (e.g. Google maps), one is able to overview the entire country, and then progressively zoom in to view Massachusetts, Amherst, and even the UMass Amherst campus, all seamlessly and within a single system.

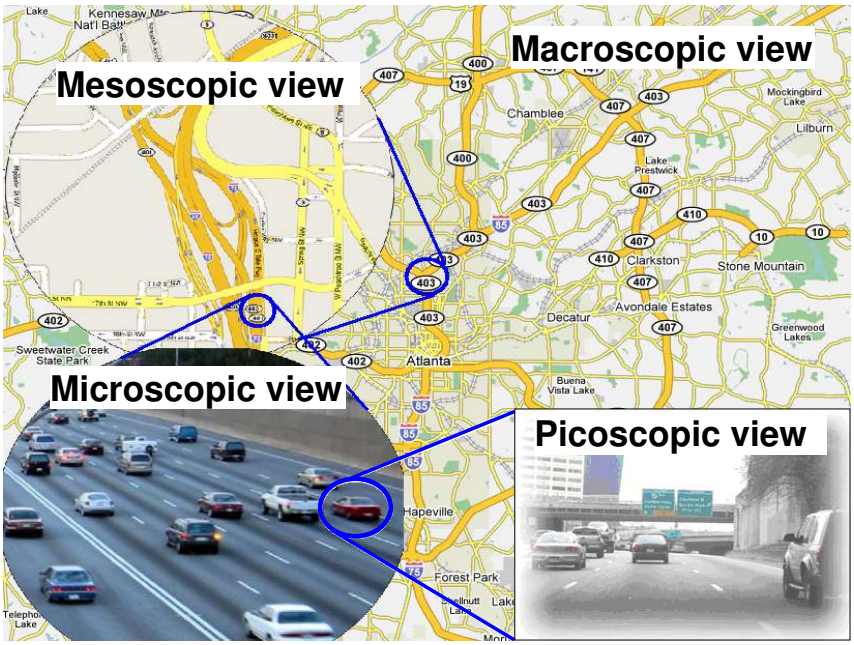

Figure 1: Multiscale traffic flow modeling

Similarly, it is desirable that traffic simulation would allow an analyst to zoom in to examine low-level details and zoom out to overview system-wide performance within the same simulation process. Figure 1 illustrates such a paradigm. The background represents a *macroscopic* view of traffic operation in an entire region. This is analogous to viewing traffic 10,000 m above the ground and the traffic appears to be a compressible fluid whose states (speed, flow, and density, etc.) propagate like waves. As one zooms in to a local area of the region, a *mesoscopic* view is obtained. This is like viewing traffic 3,000 m above the ground where the sense of waves recedes and a scene of particles emerges. As one further zooms in to a segment of the roadway, a *microscopic* view is resulted. Similar to watching traffic 1,000 m above the ground, the scene is dominated by moving particles that interact with each other so as to maintain safe positions in traffic stream. Finally, if one focuses on a few neighboring vehicles, a *picoscopic* view is achieved as if one were operating one of the vehicles. As such, one has to interact with the driving environment (e.g. roadway, signs, signals, etc.), make control decisions, and manage vehicle dynamic respond to travel safely. If such a "zoomable" simulation becomes available, one would be able to translate traffic flow representation among multiple scales, e.g. to trace a low-level event all the way to a high-level representation and, conversely, to decompose a global problem down to one or more local deficiencies. As such, the "zoomable" simulation will transform the way that traffic flow is analyzed and transportation problems are addressed.

The objective of this paper is to address multiscale traffic flow modeling with inherent consistency. The term consistency here concerns the coupling among models at different scales, i.e. how less detailed models are derived from more detailed models and, conversely, how more detailed models are aggregated to less detailed models. Only consistent multiscale models are able to provide the theoretical foundation for the above "zoomable" traffic simulation. The paper is organized as follows. Section 2 takes a broad perspective on a spectrum of four modeling scales. Modeling objectives and model properties at each scale are discussed and existing efforts are reviewed. Section 3 presents the proposed multiscale approach based on field theory. Modeling strategy at each scale is discussed and some special cases are formulated at both the microscopic and macroscopic scales. The emphasis of this multiscale approach is to ensure coupling among different modeling scales. Section 4 presents numerical and empirical results in support of the special cases developed in the previous section. Concluding remarks and future directions are presented in Section 5.

2 The Spectrum of Modeling Scales

The modeling of traffic flow can be performed at, but is not limited to, a spectrum of four scales, namely picoscopic, microscopic, mesoscopic, and macroscopic from the most to the least detailed in that order. Considering that the definition of these modeling scales are rather vague, implicit, or absent in the literature, this section attempts to provide an explicit definition so that existing and future models are easily classified and related. Such a definition is tabulated in Figure 2 for each of the four modeling scales based on their properties (i.e. rows in the table) and literature related to each modeling scale is reviewed in subsequent subsections. The first three rows ("State variable", "Variable description", and "State diagram") are discussed in this section and the remaining three rows ("Underlying principle", "Modeling approach", and "Model coupling") pertain to the proposed multiscale approach with inherent consistency which are to be elaborated in the next section.

2.1 The picoscopic scale

Picoscopic modeling should be able to represent traffic flow so that the trajectory of each vehicle, $(x_i(t), y_i(t))$ where $i \in \{1, 2, 3, ..., I\}$ denotes vehicle ID, can be tracked in both longitudinal x and lateral y directions over time $t \geq 0$. Knowing these vehicle trajectories, the state and dynamics of the traffic system can be completely determined. Therefore, $(x_i(t), y_i(t))$ is the state variable (one or a set of variables that characterizes the state of a system). The corresponding state diagram (a graphical representation that illustrates

Scale	Picoscopic	Microscopic	Mesoscopic	Macroscopic
State variable	$(x_i(t), y_i(t))$ $i = 1,2,3,\ldots \quad 0 < t < \infty$	$(x_i(t), LN_i(t))$ $LN \in \{1,2,\ldots,n\}$	$f(x,v,t)$	$k(x,t)$
Variable description	Vehicle trajectory in longitudinal x and lateral y directions	Vehicle trajectory in x direction and lane # LN in y direction	Distribution of a vehicle at location x and time t with speed v	Concentration of vehicles at location x and time t
State diagram	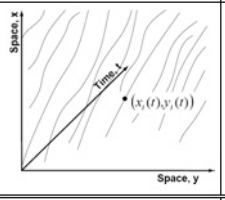	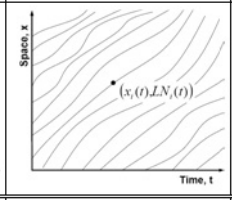	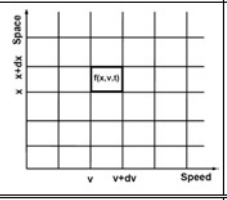	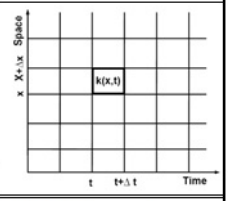
Underlying principle	Control theory System dynamics Field theory	Field theory	Statistical mechanics	Fluid dynamics
Modeling approach	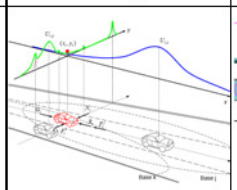	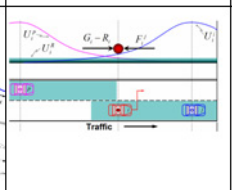	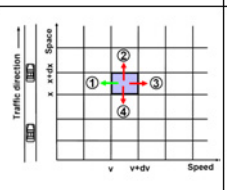	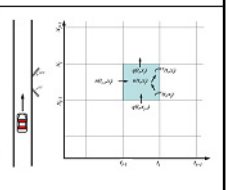
Model coupling	Pico-Micro	Micro-Meso	Meso- Macro	Micro - Macro

Figure 2: The spectrum of modeling scales

the dynamics or evolution of system state) consists of these vehicle trajectories in a three-dimensional domain (x, y, t).

Picoscopic models are mainly of interest in automotive engineering. Dynamic vehicle models with varying degrees of freedom have been proposed [1, 2]. A myriad of driver models have been reported to assist various aspects of automotive engineering including vehicle handling and stability. Control Theory was widely applied in modeling vehicle control [3, 4]. Models in this category typically incorporate one or more feedback loops. These loops are used by the controller to adjust its output to minimize control error. Human drivers can better perform reasoning using vague terms than controllers. This observation allows the use of fuzzy logic [5, 6], which controls vehicles based on some predefined rules. To allow implicit driving rules, Artificial Neural Networks [7, 8] learn "driving experiences" from training processes and then apply the learned experiences in future driving. Several literature surveys of driver models are available [9, 10, 11].

2.2 The microscopic scale

Microscopic modeling should be able to represent traffic flow so that the trajectory of each vehicle can be tracked in the longitudinal direction $x_i(t)$ with the lateral direction being discretized by lanes $LN_i(t)$ where $LN \in \{1, 2, ..., n\}$. Hence, $(x_i(t), LN_i(t))$ is state variable that describe the sate and dynamics of traffic flow at this scale and the corresponding state diagram consists of vehicle trajectories in a two-dimensional domain (x, t).

Within traffic flow community, microscopic models treat driver-vehicle units as massless particles with personalities. The behavior of these particles is governed by car-following models in the longitudinal direction and discrete choice (e.g. lane-changing and gap-acceptance) models in the lateral direction. Car-following models describe how a vehicle (the follower) responds to the vehicle in front of it (the leader). For example, stimulus-response models [12, 13] assume that the follower's response (e.g. desired acceleration) is the result of stimuli (e.g. spacing and relative speed) from the leader, desired measure models [14, 15] assume that the follower always attempts to achieve his desired gains (e.g. speed and safety), psycho-physical models [16, 17] introduce perception thresholds that trigger driver reactions, and rule-based models [18] apply "IF-THEN" rules to mimic driver decision making. Lane-changing and gap-acceptance models describe how a driver arrives at a lane change decision and how the driver executes such a decision, respectively. Approaches to lane-changing include mandatory and discretionary lane-changing (MLC/DLC) [19, 20], adaptive acceleration MLC/DLC [21, 22], and autonomous vehicle control [23]. The following have been attempted to model gap acceptance: deterministic models [24, 25, 26], probabilistic models [27, 28, 29], and neuro-fuzzy hybrid models [30]. More surveys on microscopic models can be found in the literature[31, 32].

2.3 The mesoscopic scale

Mesoscopic modeling should be able to represent traffic flow so that the probability of the presence of a vehicle at a longitudinal location x with speed v at time t is tracked. The lateral direction is only of interest if it provides passing opportunities. The state diagram typically involves a two-dimensional domain (x, v) at an instant t and the domain is partitioned into cells with space increment dx and speed increment dv. The state variable is a distribution function $f(x, v, t)$ such that $f(x, v, t)dxdv$ denotes the probability of having a vehicle within space range $(x, x + dx)$ and speed range $(v, v + dv)$ at time t. Knowing the distribution function $f(x, v, t)$, the dynamics of the system can be determined statistically.

Conventional mesoscopic traffic flow models come with three flavors. First, models such as the one in TRANSIMS [33] take a Cellular Automata approach

where the space domain (representing the longitudinal direction of a highway) is partitioned in to short segments typically 7.5 meters long. If occupied, a segment is only able to store one vehicle. Vehicles are then modeled as hopping from one segment to another, so their movement and speed are discretized and can only take some predetermined values. Second, models such as those implemented in DynaMIT [34] and DYNASMART [35] use macroscopic models (such as speed-density relationship), as oppose to microscopic car-following models, to determine vehicle speed and movement. Third, truly mesoscopic models such as the one postulated by Prigogine and his co-workers [36] are based on non-equilibrium statistical mechanics or kinetic theory which draw analogy between classical particles and highway vehicles. Prigogine's model criticized [37] for (1) lacking theoretical basis, (2) lacking realism (e.g. car following, driver preferences, and vehicle lengths), and (3) lacking satisfactory agreement with empirical data. Many efforts have been made to improve Prigogine's model by addressing critiques 2 and 3. For example, Paveri-Fontana [38] considered a driver's desired speeds, Helbing [39] adapted the desired speeds to speed limits and road conditions, Phillips [40, 41] incorporated vehicle lengths, Nelson [42] accounted for vehicle acceleration behavior, and Klar and Wegener [43, 44] included a stochastic microscopic model. Surveys of previous approaches are available in the literature[45].

2.4 The macroscopic scale

Macroscopic modeling should be able to represent traffic flow so that only local aggregation of traffic flow (e.g. density k, speed u, and flow q) over space (longitudinal) x and time t is tracked. Traffic density $k(x,t)$ is a good candidate of state variable because, unlike flow and speed, density is an unambiguous indicator of traffic condition. The state diagram typically involves a two dimensional domain (x,t). Knowing $k(x,t)$, the dynamics of the system can be determined macroscopically.

Conventional macroscopic traffic flow models describe the propagation of traffic disturbances as waves. A fundamental basis for formulating wave propagation is the law of conservation. The first-order form of the law is mass/vehicle conservation, which is used to create first-order models[46, 47]. In addition, momentum and energy may also be conserved. A model is of a higher order if it incorporates the latter forms of conservation[48, 49]. Since the limited benefit offered by higher-order models often does not justify their added complexity[50], numerical approximation and macroscopic simulation have been centered on first-order models, e.g. KRONOS[51], KWaves[52], CTM[53, 54], FREQ[55], and CORQ [56]. More surveys of macroscopic models can be found in the literature[31].

2.5 Issues of multiscale modeling

Remarkably, existing models at the same scale typically follow different modeling approaches and, hence, it is difficult to relate these models to each other. In addition, models at different modeling scales are rarely coupled. For example, a macroscopic model typically lacks a microscopic basis and a microscopic model does not have its macroscopic counterpart.

Therefore, an ideal multiscale modeling approach should emphasize not only model quality at each individual scale but also the coupling between different scales. Only models formulated following such an approach is able to support the "zoomzble" traffic simulation discussed in Section 1. As such, the resulting state diagram at a more detailed scale contains the necessary information to reproduce a less detailed diagram, as illustrated in Figure 2. For example, the microscopic diagram is simply a projection of the picoscopic diagram onto the $x - t$ plane and the macroscopic state diagram can be completely reconstructed from the microscopic diagram using Eddie's definition of traffic flow characteristics [57, 58].

3 The Proposed Multiscale Approach

The objective of this section is to pursue the above multiscale modeling approach and develop strategies to formulate a spectrum of models with inherent consistency. The approach starts at the picoscopic scale by formulating a model that is mathematically amenable to representing the natural way of human thinking while comply to physical principles; the microscopic model can be simplified from the picoscopic model yet still capturing the essential mechanisms of vehicle motion and interaction; the mesoscopic model can be derived from the microscopic model based on principles of non-equilibrium statistical mechanics; the macroscopic model can be derived from the mesoscopic model by applying principles of fluid dynamics. See a summary of underlying principle, modeling approach, and modeling coupling in Figure 2.

3.1 Picoscopic modeling

In order to conform to real-world driving experiences, the proposed model should mimic the way that a driver operates his/her vehicle and responds to the driving environment. Based on principles of control theory, a driver-vehicle-environment closed-loop control (DVECLC) system [59, 60, 61] has been developed. Figure 3 illustrates the components of the system and its control flow including feedback loops.

This system consists of a driver model and a vehicle model which interact with each other as well as with the driving environment. the driver receives

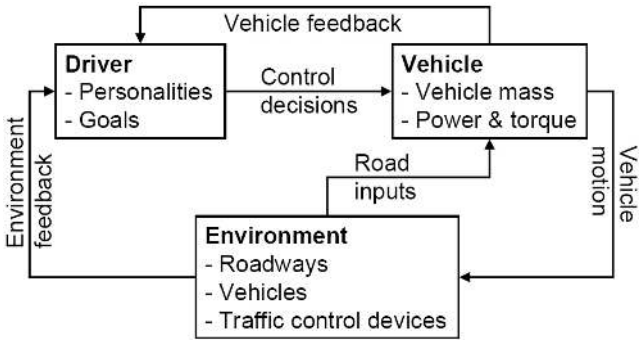

Figure 3: The closed-loop system

information from the environment such as roadways, traffic control devices, and the presence of other vehicles. The driver also receives information from his/her own vehicle such as speed, acceleration, and yaw rate. These sources of information, together with driver properties and goals, are used to determine driving strategies (such as steering and gas/brake). The driving strategies are fed forward to the vehicle which also receives input from roadways. These sources of information, together with vehicle properties, determine the vehicle's dynamic responses based on vehicle dynamic equations. Moving longitudinally and laterally, the vehicle constitute part of the environment. Other vehicle dynamic responses such as speed, acceleration, and yaw rate are fed back to the driver for determining driving strategies in the next step. Thus traffic operation is the collection of movement and interaction of all vehicles in the environment.

By applying principles of System Dynamics, a dynamic vehicle model has also been developed [62, 63] that is able to describe the dynamic response of a vehicle to its driver's control. The acceleration performance of which is shown in Figure 4. The bold line is the model output and the points are empirical data. In addition, a simple yet accurate engine model[64] was proposed to describe vehicle acceleration performance.

The driver model can be formulated by applying principles of field theory. Basically, objects in a traffic system (e.g. roadways, vehicles, and traffic control devices) are perceived by a subject driver as component fields. The driver interacts with an object at a distance and the interaction is mediated by the field associated with the object. The superposition of these component fields represents the overall hazard encountered by the subject driver. Hence, the objective of vehicle motion is to seek the least hazardous route by navigating through the field along its valley and traffic flow consists of the motion and interaction of all vehicles. With this understanding, the driver model at the picoscopic scale is formulated as follows.

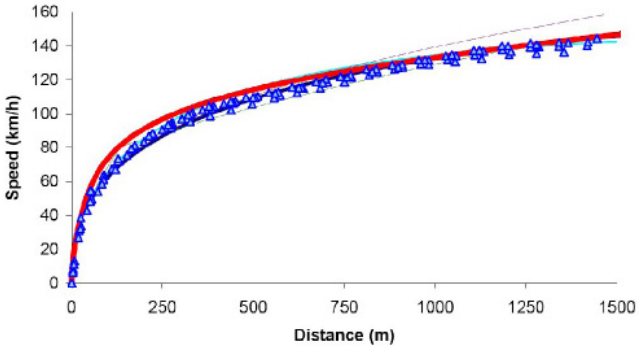

Figure 4: Vehicle model results

3.1.1 Roadways

Roadways can be represented as a gravity field in the longitudinal x direction so that vehicles are accelerated forward just like free objects fall to the ground. The gravity G_i acting on a driver-vehicle unit i can be expressed as

$$G_i = m_i \times g_i$$

where m_i is the vehicle's mass and g_i is the acceleration of roadway gravity perceived by driver i. Meanwhile, such a gravity is counteracted by a resistance R_i perceived by the driver due to her willingness to observe traffic rules (e.g. speed limit). As such, the net force

$$m_i \ddot{x}_i = G_i - R_i$$

explains the driver's unsatisfied desire for mobility which vanishes when her desired speed v_i is achieved, see an illustration in Figure 5.

In the lateral y direction, cross-section elements (e.g. lane lines, edge lines, and center lines) are perceived by the driver as a roadway potential field U_i^R. When the unit deviates from its lane, the unit is subject to a correction force N_i which can be interpreted as the stress on the driver to keep her lane. The effect of such a force is to push the vehicle back to the center of the current lane. Such a force can be derived from the roadway field as

$$N_i = -\frac{\partial U_i^R}{\partial y}$$

3.1.2 Vehicle interaction

Vehicles can each be represented as a potential field. Figure 5 illustrates two such fields perceived by driver i (the dot), one for unit j and the other for unit

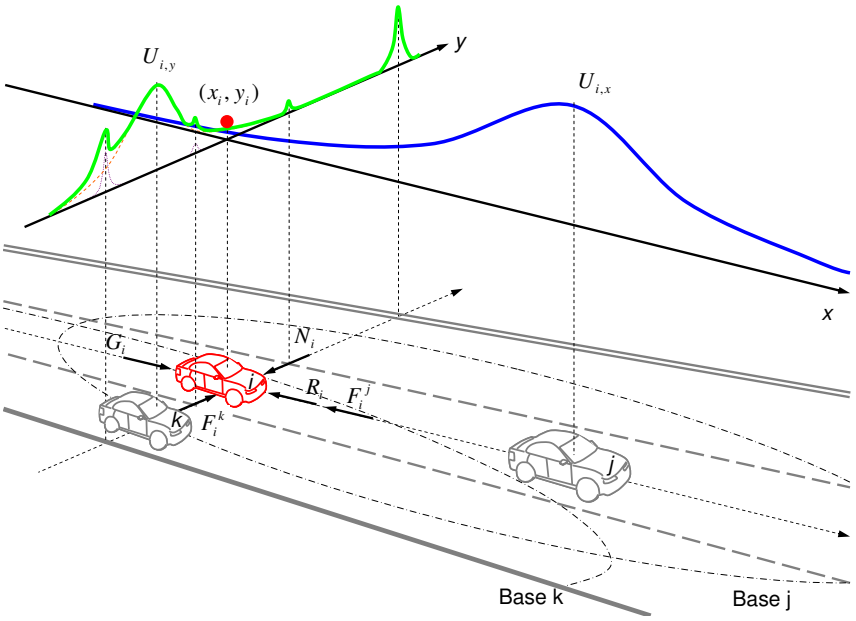

Figure 5: The illustration of a perceived field

k (the hills above and associated bases on the ground). Unit i interacts with j and k at a distance mediated by their associated fields, e.g. unit j slows down i by a repelling force F_i^j, while k motivates i to shy away by another force F_i^k where F_i^j and F_i^k can be each be derived from their corresponding fields:

$$F_i^j = -\frac{\partial U_i^j}{\partial x} \qquad F_i^k = -\frac{\partial U_i^k}{\partial y}$$

3.1.3 Traffic control devices

A red light can be represented as a potential field that appears periodically at a fixed location. When it appears, an approaching vehicle will decelerate to a stop. When the signal turns green, its field disappears and the vehicle will be accelerated by the roadway gravity. Similar technique applies to stop and yield signs with modifications accordingly. The representation of pavement markings such as lane lines, center lines, and road edges have been discussed above in representing roadways.

3.1.4 Driver's responsiveness

The above forces may or may not take effect on the subject driver depending on her responsiveness, γ. Consequently, a force that actually acts on the driver $\tilde{F}_i$ is the product of her responsiveness γ and the force that she might have

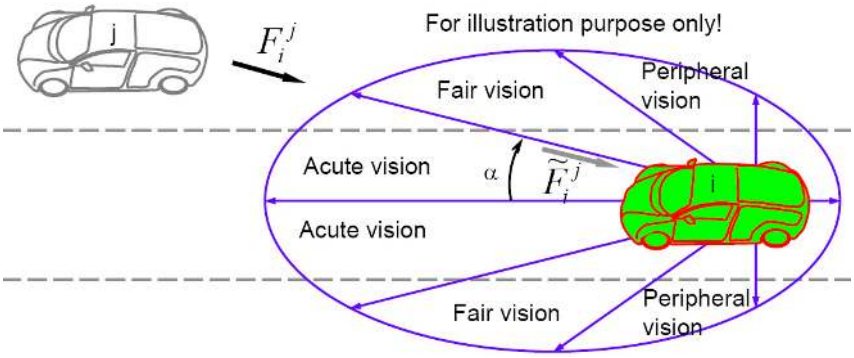

Figure 6: Driver's responsiveness

been perceived if she had paid full attention to it, F_i, i.e. $\tilde{F}_i = F_i \times \gamma$. The PI's studies on human factors [61, 65] found that the driver's responsiveness to her surroundings vary with her viewing angle $\alpha \in [-\pi, \pi]$ and scanning frequency ν, see Figure 6. For example, the front area typically receives her most attention, side areas are noted by the driver's fair or peripheral vision, and the rear area is only scanned occasionally. As such, if one chooses $\gamma(0) = 1$ and $\gamma(\pi) = 0$, the driver responds to F_i in full if it comes from a leading vehicle (i.e., $\alpha = 0$) and she ignores F_i when it comes from a trailing vehicle (i.e., $\alpha = \pi$), respectively.

3.1.5 Driver's operational control

The driver's strategy of moving on roadways is to achieve gains (mobility and safety) and avoid losses (collisions and violation of traffic rules). Such a strategy can be represented as navigating through the valley of an overall field U_i which consists of component fields such as those due to moving units U_i^B, roadways U_i^R, and traffic control devices U_i^C, i.e.

$$U_i = U_i^B + U_i^R + U_i^C$$

For example, Figure 5 illustrates two sections the overall field, $U_{i,x}$ and $U_{i,y}$. The subject unit i is represented as a ball which rides on the tail of curve $U_{i,x}$ since the vehicle is within unit j's field. Therefore, unit i is subject to a repelling force F_i^j which is derived from $U_{i,x}$ as:

$$F_i^j = -\frac{\partial U_{i,x}}{\partial x}$$

The effect of F_i^j is to push unit i back to keep safe distance. By incorporating the driver's unsatisfied desire for mobility $(G_i - R_i)$, the net force in the x direction can be determined as:

$$m_i\ddot{x}_i = \sum F_{i,x} = G_i - R_i - F_i^j = (G_i - R_i) + \frac{\partial U_{i,x}}{\partial x}$$

The section of U in the lateral y direction, $U_{i,y}$ (the bold curve), is the sum of two components: the cross section of the field due to unit k (the dashed curve) and that due to the roadway field (the dotted curve). The former results in a repelling force F_i^k which makes unit i to shy away from k and the latter generates a correction force N_i if i deviates its lane center. Therefore, the net effect can be expressed as:

$$m_i\ddot{y}_i = \sum F_{i,y} = F_i^k - N_i = -\frac{\partial U_{i,y}}{\partial y}$$

By incorporating time t, unit i's perception-reaction time τ_i, and driver i's directional response γ, the above equations can be expressed as:

$$m_i\ddot{x}_i(t+\tau_i) = \sum \tilde{F}_{i,x}(t) = \gamma_i^0[G_i(t) - R_i(t)] + \gamma(\alpha_i^j)\frac{\partial U_{i,x}}{\partial x}$$

$$m_i\ddot{y}_i(t+\tau_i) = \sum \tilde{F}_{i,y}(t) = -\gamma(\alpha_i^k)\frac{\partial U_{i,y}}{\partial y}$$

where $\gamma_i^0 \in [0,1]$ represents the unit's attention to its unsatisfied desire for mobility (typically $\gamma_i^0 = 1$), α_i^j, α_i^k, and α_i^N are viewing angles which are also functions of time.

3.2 Microscopic modeling

The microscopic model can be formulated by simplifying the above picoscopic model as follows: (a) ignoring interactions inside a driver-vehicle unit allowing it to be modeled as an active particle, (b) representing a driver's longitudinal and lateral control using separate but simpler models, (c) reducing the vehicle dynamic system to a particle, and (d) simplifying roadway surfaces to a collection of lines.

3.2.1 Modeling longitudinal control

With the above simplifications, the two-dimensional (3D) potential field U in Figure 5 reduces to a 2D potential function. The upper part of Figure 7 illustrates an example where a subject driver i (the middle one) is traveling behind a leading vehicle j and followed by a third vehicle p in the adjacent lane. The potential field U_i perceived by the driver is shaded in the lower part of the figure and is represented by a curve in the upper part. Since the trailing vehicle in the adjacent lane does not affect the subject driver's longitudinal motion, the "stress" on the subject driver to keep safe distance only comes from the leading vehicle and can be represented as:

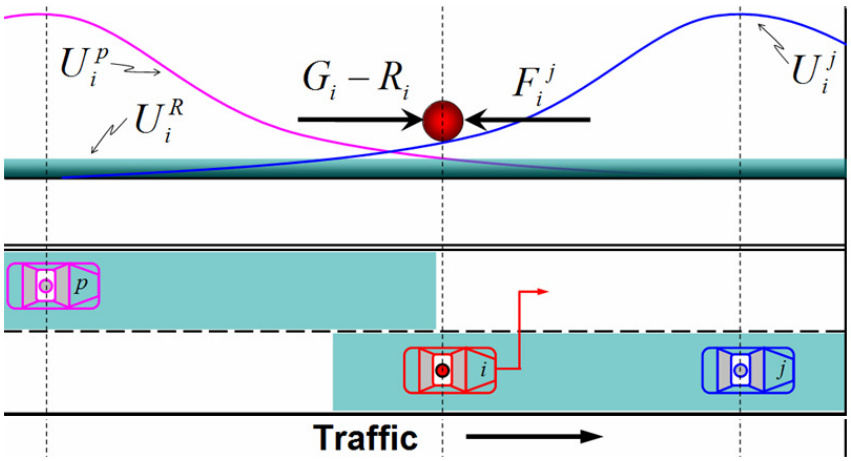

Figure 7: Microscopic modeling

$$F_i^j = -\frac{\partial U_i^j}{\partial x}$$

By incorporating roadway gravity G_i, roadway resistance R_i, and interaction between vehicles F_i^j, the net force on i can be expressed more specifically as:

$$m_i \ddot{x}_i = G_i - R_i - F_i^j$$

Departing from the above equation, a few special cases deserve particular attention:

$$\ddot{x}_i(t+\tau_i) = g_i[1 - (\frac{\dot{x}_i(t)}{v_i}) - e^{\frac{s_{ij}(t)^* - s_{ij}(t)}{s_{ij}(t)^*}}] \tag{1}$$

$$\ddot{x}_i(t+\tau_i) = g_i[1 - (\frac{\dot{x}_i(t)}{v_i}) - e^{\frac{s_{ij}(t)^* - s_{ij}(t)}{v_i \tau_i}}] \tag{2}$$

$$\ddot{x}_i(t+\tau_i) = g_i[1 - (\frac{\dot{x}_i(t)}{v_i}) - 2(1 - \frac{1}{1 + e^{\frac{s_{ij}(t)^* - s_{ij}(t)}{v_i \tau_i / 2 + L_j}}})] \tag{3}$$

where it is assumed that $G_i = m_i \times g_i$, $R_i = m_i \times (\frac{\dot{x}_i(t)}{v_i})$, $F_i^j = m_i \times f(s_{ij}, s_{ij}(t)^*)$, g_i is the maximum acceleration that driver i is willing to apply when starting from stand still, $\dot{x}_i(t)$ is the actual speed of vehicle i, v_i is the desired speed of driver i, $s_{ij} = x_j - x_i$ is the actual spacing between vehicles i and j, x_i is the position of vehicle i, x_j is the position of vehicle j, s_{ij}^* is the desired spacing between vehicles i and j. L_j is the nominal length of vehicle j and is conveniently used as the spacing between two vehicles in jammed traffic. The the difference $(s_{ij}^* - s_{ij})$ represents how far vehicle i intrudes beyond s_{ij}^*.

The rationale of representing the interaction force F_i^j between vehicles i and j using an exponential function is to set the desired spacing s_{ij}^* as a base line, beyond which the intrusion by unit i is translated exponentially to the repelling force acting on the unit. The desired spacing s_{ij}^* can be further determined as follows.

According to [15], the desired spacing should allow vehicle i to stop behind its leading vehicle j after a perception-reaction time τ_i and a deceleration process at a comfortable level $b_i > 0$ should vehicle j applies an emergency brake at rate $B_j > 0$. This rule results in

$$s_{ij}^*(t) = x_{i-1}(t) - x_i(t) \geq \frac{\dot{x}_i^2(t)}{2b_i} + \dot{x}_i\tau_i - \frac{\dot{x}_{i-1}^2(t)}{2B_{i-1}} + L_j$$

Alternatively, one may choose to set the desired spacing as a simplified function of the relative speed of the two vehicles:

$$s_{ij}^*(t) = L_j + L_j(\dot{x}_i(t) - \dot{x}_j(t))$$

3.2.2 Modeling lateral control

The driver's lateral control concerns changing lanes to seek a speed gain or to use an exit. The shaded areas in the bottom part of Figure 7 can be interpreted as drivers j and p's personal spaces after accounting for lane barrier. A lane change decision is reached whenever driver i intrudes into another driver's personal space. With such a decision, driver i begins to search for open spaces in adjacent lanes. In this particular case, such an open space happens to be available in the left lane barely allowing the center of vehicle i to move in. Consequently, the result of the gap acceptance decision is to abruptly switch vehicle i to the left lane.

3.3 Mesoscopic modeling

Mesoscopic modeling applies principles of Non-Equilibrium Statistical Mechanics or kinetic theory to model traffic flow. Essential to the modeling is the determination of a distribution function $f(x, v, t)$ such that $f(x, v, t)dxdv$ denotes the probability of having a vehicle within space range $(x, x + dx)$ and speed range $(v, v + dv)$ at time t (see Figure 8). The time evolution of traffic flow is described by an evolution equation

$$\frac{df}{dt} = \frac{\partial f}{\partial t} + \frac{\partial f}{\partial x}\frac{dx}{dt}$$

whose right-hand side is to be determined. Therefore, the central question is how to rigorously derive the evolution equation. This can be done by following

a procedure similar to deriving the Boltzmann equation [66, 67] from basic principles. The classical Boltzmann equation describes particles moving in a 3D domain, so the first step is to reduce the 3D case to a 1D case which represents traffic moving on a unidirectional highway.

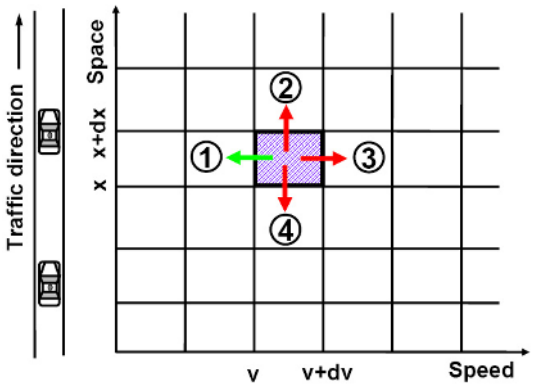

Figure 8: The x-v diagram

Existing models, in particular those based on Prigogine's work, are postulated. In order to derive the 1D Boltzmann equation from basic principles, a sound understanding of the mechanism of traffic evolution is required. Existing models, including a derived model [43, 44], assumed that the mechanism is vehicle "collision". For example, the fast follower i in the left panel of Figure 9) keeps its speed up to the collision point and then abruptly changes its speed. To be realistic, the speed change of vehicle i needs to be smooth as it approaches its leader j as illustrated in the right panel of Figure 9). This is possible only if car following is incorporated as the mechanism of particle interaction. As such, the longitudinal control model presented above can be used to derive the 1D Boltzmann equation and, thus, ensures micro-meso coupling.

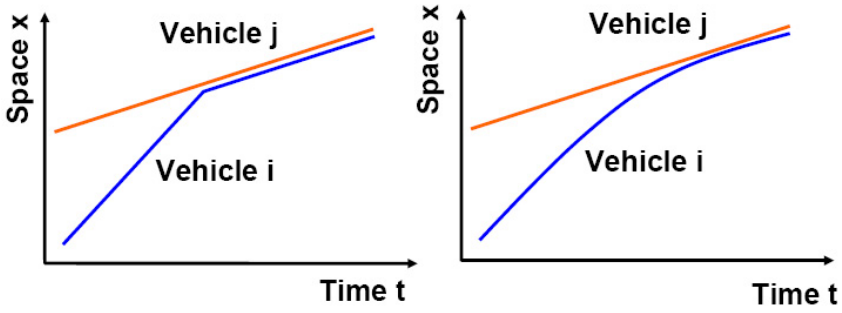

Figure 9: Car following

The derivation of the 1D Boltzmann equation starts by applying conservation law (e.g vehicles entering and exiting the highlighted cell in Figure 8

should be conserved). Existing models considered only one direction (i.e. direction 1 below) in which vehicles exit the cell, and a similar treatment applies to vehicles entering the cell. This approach causes modeling errors. Actually, vehicles may exit the cell in four directions: (1) vehicles slowed down (and hence exited the cell) due to a sluggish leader, (2) vehicles physically moved out of the cell, (3) vehicles accelerated by an aggressive follower, and (4) vehicles reversed, which is unlikely. The opposite applies to vehicles entering the cell. Therefore, applying the law to include all directions is the correct approach. Since deriving the 1D Boltzmann equation is mathematically complicated, this paper only presents potential directions of exploration, leaving the actual derivation to be addressed in future research.

Once the 1D Boltzmann equation is formulated, one may solve it based on initial and boundary conditions to study how traffic evolves over time and space. However, solving the equation can be quite involved, as is the case for any classical Boltzmann equation. Fortunately, some important results can be inferred without fully solving the equation. For example, a hydrodynamical formulation, which is essential to macroscopic modeling, can be derived from the equation. In addition, the equation contains an equilibrium relationship between vehicle speed and traffic density, which is also essential to macroscopic modeling. Such a relationship is analogous to the Maxwell-Boltzmann distribution (the distribution of molecular speed under different temperature) which is the stationary (i.e. $\frac{\partial f}{\partial t} = 0$) solution to a classical Boltzmann equation.

3.4 Macroscopic modeling

Macroscopic modeling applies principles of Fluid Dynamics to model traffic flow as a 1D compressible continuum fluid. While the above mesoscopic modeling describes the distribution of vehicles in a highway segment, macroscopic modeling represents only the average state. Therefore, traffic density $k(x,t)$ can be related to the distribution $f(x,v,t)$ as its zeroth moment $k(x,t) = \int f(x,v,t)dv$ and traffic speed as the first moment $u(x,t) = \frac{1}{k}\int vf(x,v,t)dv$. Based on this understanding, it becomes clear that it is feasible to derive a hydrodynamical formulation from the mesoscopic model. The 1D Boltzmann equation discussed above can be expressed in a general form as

$$\frac{\partial f}{\partial t} + v\frac{\partial f}{\partial x} = C$$

where C denotes the rate of change of $f(x,v,t)$. Multiplying both sides of this equation by 1, v, and $\frac{1}{2}v^2$ and integrating over v will give hydrodynamical equations of mass, momentum, and energy conservation. The mass conservation equation

$$\frac{\partial k}{\partial t} + \frac{\partial (ku)}{\partial x} = \int C dv$$

is of particular interest because it describes the time evolution of traffic density $k(x,t)$. In order to solve the equation, a speed-density relationship must be introduced into the macroscopic model. This relationship can be derived from the mesoscopic model under stationary conditions or, alternatively, obtained directly from the microscopic model by assuming equilibrium conditions. Presented below are a set of equilibrium v-k relationships derived from the special cases of the microscopic model, respectively:

$$v = v_f[1 - e^{1-\frac{k^*}{k}}] \tag{4}$$

$$v = v_f[1 - e^{1-\frac{1/k_j - 1/k}{v_f \tau}}] \tag{5}$$

$$v = v_f[\frac{2}{1 + e^{\frac{1/k_j - 1/k}{v_f \tau/2 + 1/k_j}}} - 1] \tag{6}$$

where $k^* = \tau v e^{-\frac{v}{v_f}} + \frac{1}{k_j}$, v_f is free-flow speed, $k_j = 1/L$, L is the bumper-to-bumper distance between vehicles when traffic is jammed, τ is average perception-reaction time of drivers.

Therefore, the macroscopic model consists of a system of equations including the hydrodynamical formulation and one of the above speed-density relationships.

$$\frac{\partial k}{\partial t} + \frac{\partial ku}{\partial x} = \int C dv$$
$$v = V(k)$$

The the system of equations can be solved using a finite difference method. A typical finite difference method is illustrated in Figure 10 where one partitions the time-space domain into cells and keeps track of traffic flowing into and out of each cell [68, 51, 69].

4 Empirical and Numerical Results

This section provides some empirical and numerical evidences in support of the proposed multiscale approach. Particular attention is devoted to microscopic models such as the special cases proposed in Subsection 3.2 and their corresponding speed-density relationships presented in Subsection 3.4.

At the microscopic level, the emphasis is to check if a model makes sense since it is not reasonable to expect the same result out of a simulated run and a real one due to randomness. A physically meaningful scenario is set up as follows which consists of multiple regimes typically encountered during driving. The scenario involves two vehicles, a leader and a follower. The leader moves according to predetermined rules, while the motion of the follower is

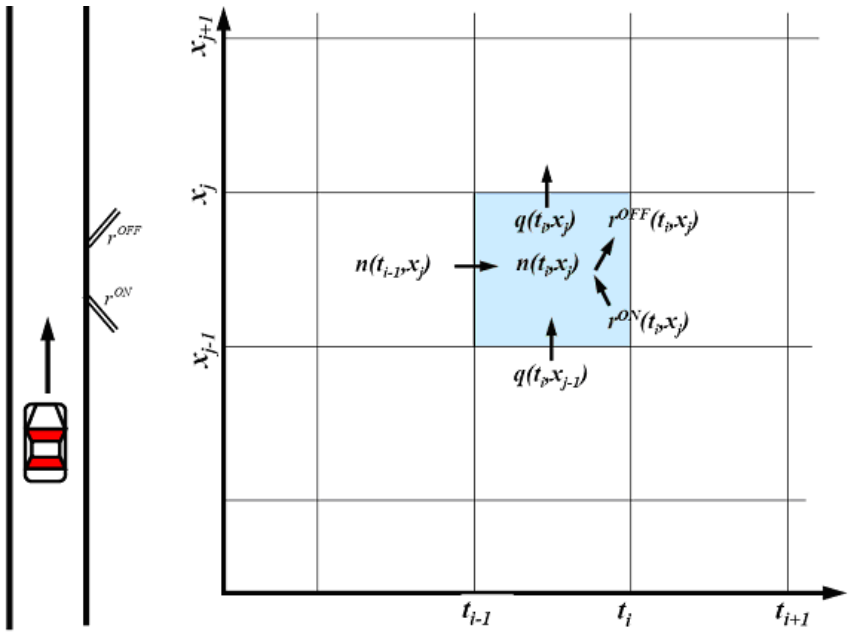

Figure 10: The finite difference method

stipulated by a microscopic model. More specifically, the follower i is initially stand still at $x_i(0) = 0$. The motion of the leader j is defined as follows:

when $0 \leq t < 100$: $x_j = 5000, \dot{x}_j = 0, \ddot{x}_j = 0$
when $t = 100$: $x_j = 2800, \dot{x}_j = 25$
when $100 \leq t < 200$: $\ddot{x}_j = 0$
when $200 \leq t < 210$: $\ddot{x}_j = 2$
when $210 \leq t < 300$: $\ddot{x}_j = 0$
when $300 \leq t < 315$: $\ddot{x}_j = -3$
when $t \geq 315$: $\ddot{x}_j = 0$

where time t is in seconds (s), displacement x is in meters (m), speed $\dot{x}$ is in m/s, and acceleration $\ddot{x}$ is in m/s^2. The above set up essentially means the following. Initially, both vehicles are stand still with the follower at $x_i(0) = 0$ m and the leader in front at $x_j(0) = 5000$ m. At time $t = 100$ s, a third vehicle in the adjacent lane traveling at 25 m/s cuts in front of the follower i at $x = 2800$ m. As such, this third vehicle takes over as the leader j and it keeps its speed constant up to $t = 200$ s. Then, the leader begins to accelerate at a constant rate of 2 m/s^2 for 10 seconds, which results in an ending speed of 45 m/s. After this, the leader cruises at that speed up to $t = 300$ s. Next, the leader applies a constant deceleration at a rate of -3 m/s^2 for 15 seconds, which essentially brings the vehicle to a stop.

The following analysis assumes a normal driver who responds based on

common sense. When the process starts, vehicle i begins to move according to the logic stipulated in the microscopic model. Since vehicle j is far away, it essentially has no influence on vehicle i who is entitled to accelerate to its desired speed $\dot{x}_i(t) \to v_i = 25\ m/s$. This process constitutes a free-flow regime. Right before $t = 100\ s$, the follower is at somewhere around $x = 2745\ m$ and the leader is 2255 m ahead. However, at $t = 100\ s$, the third vehicle cuts in right in front at $x = 2800\ m$ taking over as the new leader and shortening the inter-vehicle distance (i.e. spacing s_{ij}) to 55 m. The sudden change in spacing causes the the follower to take emergency brake in order to maintain safe distance away from its leader. This process constitutes a braking regime. The emergency brake slows down the follower and the spacing between the two vehicles increases. When safe distance is achieved, the follower begins catch up with the leader's speed and maintain the safe distance thereafter. This constitutes a car-following regime. Starting from $t = 200\ s$, the leader begins to accelerate and eventually cruises at 45 m/s. As the leader speeds up, the spacing increases allowing the follower to accelerate as well. Since the leader travels much faster than the follower and the gap is opening, the follower is entitled to accelerate as desired and eventually settles at its desired speed $v_i = 30\ m/s$. This returns to the free-flow regime again. Note that the leader's cruise speed is an exaggeration which is made on purpose to highlight the effect that the follower does not blindly follow its leader beyond its desired speed. At $t = 300\ s$, the leader begins to decelerate at comes to a stop at $x_j = 10000\ m$ after 15 seconds. As the follower approaches the stopped leader, the follower begins to decelerate, too, at a comfortable rate and finally rests right behind the leader. This process constitutes a transition from a approaching regime to the braking regime.

Figure 11 shows the performance of the special case 1 formulated in Eq. (1). Three profiles are illustrated: displacement, speed, and acceleration. Broken red lines are for the leader whose motion is predetermined as above, while solid blue lines are for the follower whose motion is stipulated by the model. Examination of the follower's performances in the free-flow, approaching, car-following, braking regimes reveals that the model does conform to the above common sense analysis. Special cases 2 (Eq. (2)) and 3 (Eq. (3)) yield similar results and are not repeated here.

At the macroscopic level, the emphasis is to compare the simulated results against empirical observations across many vehicles and over time. The empirical data is collected from GA 400 by Georgia NAVIGATOR system. The resulting speed vs density, flow vs density, and speed vs flow plots are illustrated as dots in Figure 12. Solid blue lines show the performance of macroscopic special case 1 (Eq. (4)) which is derived from Eq. (1) with the following parameters: free-flow speed $v_f = 29$ m/s, average perception-reaction time $\tau = 1.3$ s, and jam density $k_j = 1/5$ veh/m. The plots show that the

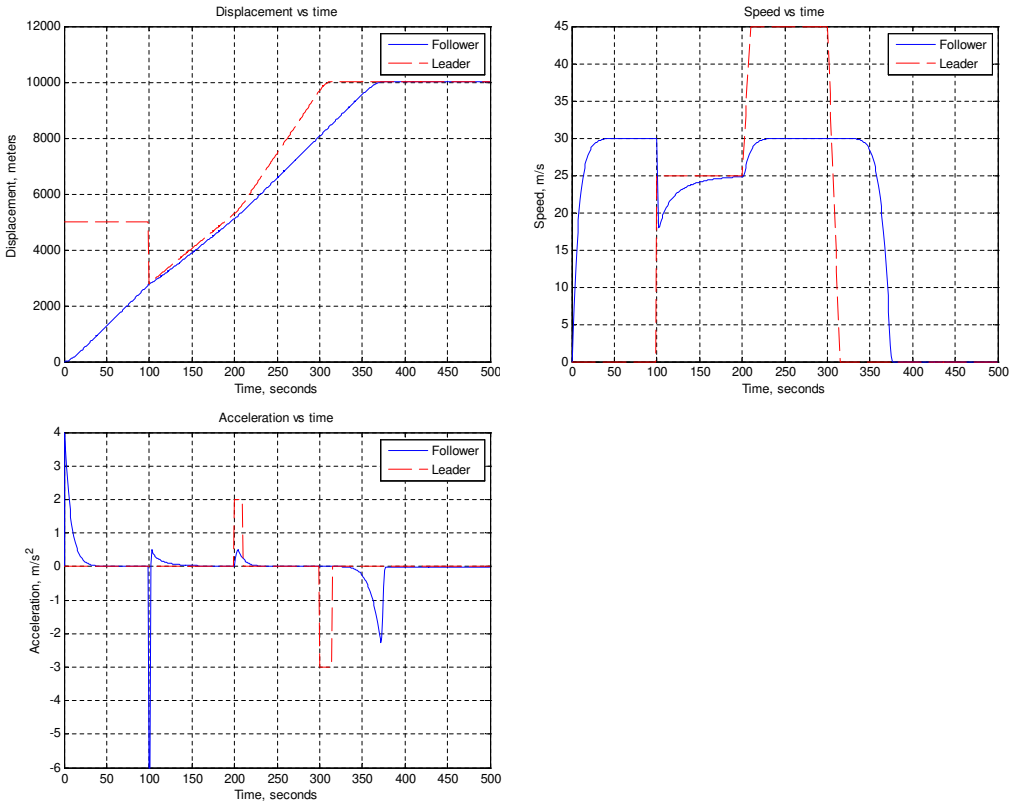

Figure 11: Performance of microscopic model special case 1 (Eq. (1))

model agrees empirical observations very well. The other two special cases performs similarly and are not repeated here.

5 Conclusion and Future Directions

This paper presents a broad perspective on traffic flow modeling at a spectrum of four scales: picoscopic, microscopic, mesoscopic, and macroscopic from the most to the least detailed level in that order. Modeling objectives and model properties at each scale are discussed and existing efforts are reviewed.

In order to ensure modeling consistency and provide a microscopic basis for macroscopic models, it is critical to address the coupling among models at different scales, i.e. how less detailed models are derived from more detailed models and, conversely, how more detailed models are aggregated to less detailed models. With this understanding, a consistent modeling approach is proposed based on field theory. Basically, in this approach, physical world objects (e.g. roadways, vehicles, and traffic control devices) are perceived by the subject driver as component fields. The driver interacts with an object

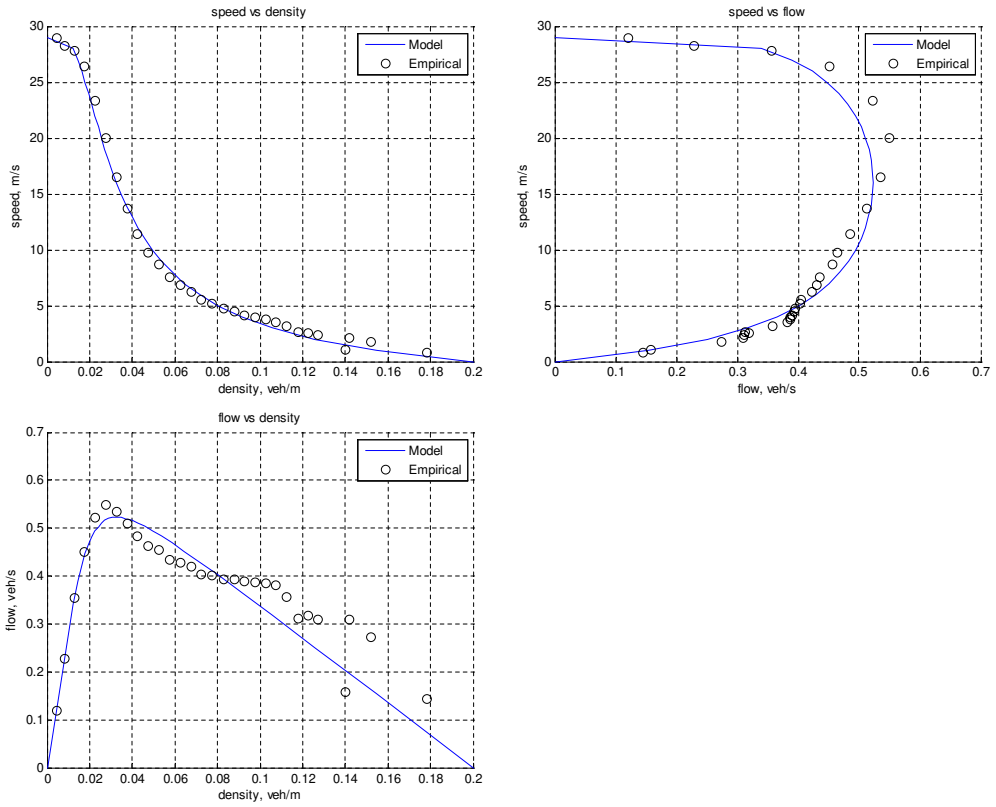

Figure 12: Performance of macroscopic model special case 1 (Eq. (4))

at a distance and the interaction is mediated by the field associated with the object. In addition, the field may vary when perceived by different drivers depending on their characteristics such as responsiveness and perception-reaction time. The superposition of these component fields represents the overall hazard encountered by the subject driver. Hence, the objective of vehicle motion is to seek the least hazardous route by navigating through the field along its valley. Consequently, traffic flow is modeled as the motion and interaction of all vehicles.

Modeling strategies at each of the four scales are discussed. More specifically, the field theory serves as the basis of picoscopic modeling which represents a driver-vehicle unit as driver-vehicle-environment closed-loop control system. The system is able to capture vehicle motion in longitudinal and lateral directions. The microscopic model is obtained from the picoscopic model by simplifying its driver-vehicle interactions, vehicle dynamics, and vehicle lateral motion. The mesoscopic model is derived from basic principles using the microscopic model as the mechanism of traffic evolution. The macroscopic model includes an evolution equation (which is derived by taking moments of the mesoscopic model) and an equilibrium speed-density relationship (which

is the stationary solution to the mesoscopic model or derived from the microscopic model directly). Therefore, the proposed approach ensures model coupling and modeling consistency. As such, consistent models drived from this approach are able to provide the theoretical foundation to develop the "zoomable" traffic simulation tool discussed in Section 1.

A few special cases of the microscopic model are formulated. Further, their corresponding equilibrium speed-density relationships are derived. A numerical test is devised to verify if these microscopic special cases make any sense. In addition, the equilibrium relationships are validated against empirical data. Both numerical and empirical results suggest that these special cases perform satisfactorily and aggregate to realistic macroscopic behavior.

This paper emphasizes modeling strategies at the four scales. Though a family of special cases are formulated at the microscopic and macroscopic scales, further efforts are needed to complete the spectrum by adding specific models at the picoscopic and mesoscopic scales. In addition, with the rapid development of wireless technologies and the deployment of IntelliDrive^{SM} initiative, the effects of vehicle-vehicle and vehicle-roadside communications will transform the way a transportation system operates. Therefore, it is desirable that traffic flow models are able to incorporate such effects to realistically simulate IntelliDrive^{SM}-enabled transportation systems.

References

[1] Masato Abe. Theoretical Analysis on Vehicle Cornering Behaviours in Braking and in Acceleration. *Vehicle System Dynamics*, 14(1-3):140–143, 1985.

[2] Erik M. Lowndes and J.W. David. Development of an Intermediate Degree of Freedom Vehicle Dynamics Model for Optimal Design Studies. *American Society of Mechanical Engineers, Design Engineering Division (Publication) DE*, 106:19–24, 2000.

[3] W.W. Wierwille, G.A. Gagne, and J.R. Knight. An Experimental Study of Human Operator Models and Closed-Loop Analysis Methods for High-Speed Automobile Driving. *IEEE Transactions on Human Factors in Electronics*, HFE-8(3):187–201, 1967.

[4] T.J. Gordon and M.C. Best. On the Synthesis of Driver Inputs for the Simulation of Closed-Loop Handling Manoeuvres. *International Journal of Vehicle Design*, 40(1-3):52–76, 2006.

[5] U. Kramer and G. Rohr. A Model of Driver Behaviour. *Ergonomics*, 25(10):891–907, 1982.

[6] Zhenhai Gao, Nanning Zheng, Hsin Guan, and Konghui Guo. Application of Driver Direction Control Model in Intelligent Vehicle's Decision and Control Algorithm. In *Intelligent Vehicle Symposium, 2002. IEEE*, volume 2, pages 413–418, 2002.

[7] Charles C. Macadam and Gregory E. Johnson. Application of Elementary Neural Networks and Preview Sensors for Representing Driver Steering Control Behaviour. *Vehicle System Dynamics*, 25(1):3–30, 1996.

[8] Y. Lin, P. Tang, W.J. Zhang, and Q. Yu. Artificial Neural Network Modelling of Driver Handling Behaviour in a Driver-Vehicle-Environment System. *International Journal of Vehicle Design*, 37(1):24–45, 2005.

[9] A.G. Zadeh, A. Fahim, and M. El-Gindy. Neural Network and Fuzzy Logic Applications to Vehicle Systems: Literature Survey. *International Journal of Vehicle Design*, 18(2):132–193, 1997.

[10] Marita Irmscher, Thomas Jurgensohn, and Hans-Peter Willumeit. Driver Models in Vehicle Development. *Vehicle System Dynamics*, 33(Suppl):83–93, 1999.

[11] Charles C. Macadam. Understanding and Modeling the Human Driver. *Vehicle System Dynamics*, 40(1-3):101–134, 2003.

[12] R.E. Chandler, R. Herman, and E.W. Montroll. Traffic Dynamics: Studies in Car Following. *Operations Research*, 6:165–184, 1958.

[13] D. C. Gazis, R. Herman, and R. W. Rothery. Non-Linear Follow the Leader Models of Traffic Flow. *Operations Research*, 9:545–567, 1961.

[14] L. A Pipes. An Operational Analysis of Traffic Dynamics. *Journal of Applied Physics*, 24:271–281, 1953.

[15] P.G. Gipps. A Behavioral Car Following Model for Computer Simulation. *Transportation Research, Part B*, 15:105–111, 1981.

[16] R. M. Michaels. Perceptual Factors in Car Following. In *Proceedings of the 2nd International Symposium on the Theory of Road Traffic Flow (London, England), OECD*, 1963.

[17] R. Wiedemann. *Simulation des Straenverkehrsflusses*. PhD thesis, Schriftenreihe des Instituts fr Verkehrswesen der Universitt Karlsruhe, Germany, 1974.

[18] I. Kosonen. *HUTSIM - Urban Traffic Simulation and Control Model: Principles and Applications*. PhD thesis, Helsinki University of Technology, 1999.

[19] P.G. Gipps. A Model for the Structure of Lane-Changing Decisions. *Transportation Research, Part B*, 20:403–414, 1986.

[20] K.I. Ahmed, M. Ben-Akiva, H.N. Koutsopoulos, and R.G. Mishalani. Models of Freeway Lane-changing and Gap Acceptance Behavior. In *Proceedings of the 13th International Symposium on the Theory of Traffic Flow and Transportation*, pages 501–515, 1996.

[21] P. Hidas and K. Behbahanizadeh. Microscopic simulation of lane changing under incident conditions. In *Proceedings of the 14th International Symposium on the Theory of Traffic Flow and Transportation*, pages 53–69, 1999.

[22] Y. Zhang, L.E. Owen, and J.E. Clark. A Multi-regime Approach for Microscopic Traffic Simulation. In *77th Transportation Research Board Annual Meeting*, 1998.

[23] Rahul Sukthankar. *Situation Awareness for Tactical Driving*. PhD thesis, Carnegie Mellon University, 1997.

[24] M.S. Raff and J.W. Hart. A Volume Warrant for Urban Stop Signs. Technical report, Eno Foundation for Highway Traffic Control, Saugatuck, Connecticut, 1950.

[25] S. M. Velan and M. Van Aerde. Gap Acceptance and Approach Capacity at Unsignalized Intersections. *ITE Journal*, 66(3):40–45, 1996.

[26] M.M. Hamed, S.M. Sama, and R.R. Batayneh. Disaggregate Gap-Acceptance Model for Unsignalised T-Intersections. *Journal of Transportation Engineering, ASCE*, 123(1):36–42, 1997.

[27] R. Herman and G.H. Weiss. Comments on the Highway Crossing Problem. *Operations Research*, 9:838–840, 1961.

[28] D.R. Drew, L.R. LaMotte, J.H. Buhr, and J.A. Wattleworth. Gap Acceptance in the Freeway Merging Process. Technical report, Texas Transportation Institute, 430-432, 1967.

[29] R.H. Hewitt. Using Probit Analysis with Gap Acceptance Data. Technical report, Department of Civil Enginneering, University of Glasgow, 1992.

[30] Riccardo Rossi and Claudio Meneguzzer. The Effect of Crisp Variables on Fuzzy Models of Gap-Acceptance Behaviour. In *Proceedings of the 13th Mini-EURO Conference: Handling Uncertainty in the Analysis of Traffic and Transportation Systems*, 2002.

[31] Nathan Gartner, Carroll J. Messer, and Ajay K. Rathi. *Revised Monograph of Traffic Flow Theory: A State-of-the-Art Report*. Transportation Research Board, 2001.

[32] S.P. Hoogendoorn and P.H.L. Bovy. State-of-the-art of Vehicular Traffic Flow Modelling. *Proceedings of the IMechE Part I, Journal of Systems and Control Engineering*, 215(4):283–303, 2001.

[33] L. Smith, R. Beckman, D. Anson, K. Nagel, and M.E. Williams. TRANSIMS: Transportation Analysis and Simulation System. In *Fifth National Conference on Transportation Planning Methods Applications-Volume II*, 1995.

[34] M. E. Ben-Akiva, M. Bierlaire, H. Koutsopoulos, and R. Mishalani. DynaMIT: A Simulation-Based System for Traffic Prediction. DACCORS Short Term Forecasting Workshop, 1998.

[35] G.-L. Chang, T. Junchaya, and A. J. Santiago. A Real-Time Network Traffic Simulation Model for ATMS Applications: Part ISimulation Methodologies. *Journal of Intelligent Transportation Systems*, 1(3):227241, 1994.

[36] I. Prigogine. *A Boltzmann-like Approach to the Statistical Theory of Traffic Flow*. Theory of traffic Flow. Elsevier, Amsterdam, 1961.

[37] F.A. Haight. Vehicles as Particles. (Book Reviews: Kinetic Theory of Vehicular Traffic by Prigogine and Herman). *Science*, 173(3996):513, 1971.

[38] S.L. Paveri-Fontana. On Boltzmann-like Treatments for Traffic Flow: A Critical Review of the Basic Model and an Alternative Proposal for Dilute Traffic Analysis. *Transportation Research*, 9:225–235, 1975.

[39] Dirk Helbing. Theoretical Foundation of Macroscopic Traffic Models. *Physica A: Statistical and Theoretical Physics*, 219(3-4):375–390, 1995.

[40] W.F. Phillips. Kinetic Model for Traffic Flow. Technical report, Report DOT/RSPD/DPB/50-77/17. U. S. Department of Transportation, 1977.

[41] W.F Phillips. A Kinetic Model for Traffic Flow with Continuum Implications. *Transportation Planning and Technology*, 5:131–138, 1979.

[42] P. Nelson. A Kinetic Model of Vehicular Traffic and its Associated Bimodal Equilibrium Solutions. *Transport Theory and Statistical Physics*, 24:383–409, 1995.

[43] R. Wegener and A. Klar. A Kinetic Model for Vehicular Traffic Derived from a Stochastic Microscopic Model. *Transport Theory and Statistical Physics*, 25:785–798, 1996.

[44] A. Klar and R. Wegener. A Hierarchy of Models for Multilane Vehicular Traffic (Part I: Modeling and Part II: Numerical and Stochastic Investigations). *SIAM Journal on Applied Mathematics (SIAP)*, 59:983–1011, 1999.

[45] Dirk Helbing. Traffic and Related Self-Driven Many-Particle Systems. *Reviews of Modern Physics*, 73:1067–1141, 2001.

[46] M. Lighthill and G. Whitham. On Kinematic Waves II. A Theory of Traffic Flow on Long Crowded Roads. *Proc. Royal Society of London, Part A*, 229(1178):317–345, 1955.

[47] P.I. Richards. Shock Waves on the Highway. *Operations Research*, 4:42–51, 1956.

[48] H.J. Payne. Models of Freeway Traffic and Control. In *Simulation Council Proceedings*, volume 1, pages 51–61, 1971.

[49] G.B. Whitham. *Linear and Nonlinear Waves*. John Wileyand Sons Inc, New York, NY., 1974.

[50] C.F. Daganzo. Requiem For Second-order Fluid Approximations of Traffic Flow. *Transportation Research B*, 29(4):277–286, 1995.

[51] P.G. Michalopoulos. Dynamic Freeway Simulation Program for Personal Computers. *Transportation Research Record*, 971:68–79, 1984.

[52] G.F. Newell. A Simplified Theory on Kinematic Waves in Highway Traffic, Part II: Queueing at Freeway Bottlenecks. *Transportation Research B*, 27(4):289–303, 1993b.

[53] C.F. Daganzo. The Cell Transmission Model: A Dynamic Representation of Highway Traffic Consistent with the Hydrodynamic Theory. *Transportation Research B*, 28(4):269–287, 1994.

[54] C.F. Daganzo. The Cell Transmission Mode, Part II: Network Traffic. *Transportation Research B*, 29(2):79–93, 1995.

[55] A.D. May. FREQ User Manual. Technical report, California Department of Transportation, Berkeley, 1998.

[56] S. Yager. CORQ - A Model for Predicting Flows and Queues in a Road Corridor. *Transportation Research Record*, 533:77–87, 1975.

[57] L.C. Eddie. Discussion on Traffic Stream Measurements and Definitions. In *Proc. 2nd International Symposium of the Theory of Traffic Flow, Paris, France*, page 139154, 1963.

[58] Daiheng Ni. Determining Traffic Flow Characteristics by Definition for Application in ITS. *IEEE Transactions on Intelligent Transportation Systems*, 8(2):181–187, 2007.

[59] Daiheng Ni. Challenges and Strategies of Transportation Modeling and Simulation under Extreme Conditions. *International Journal of Emergency Management (IJEM)*, 3(4):298–312, 2006.

[60] Daiheng Ni. A Framework for New Generation Transportation Simulation. In *Proceedings of Winter Simulation Conference '06*, Portola Plaza Hotel, Monterey, CA, December 3-6, 2006.

[61] Daiheng Ni. 2DSIM: A Prototype of Nanoscopic Traffic Simulation. In *Proceedings of the 2003 Intelligent Vehicles Symposium (IV 2003)*, pages 47–52, Columbus, OH, 2003.

[62] Dwayne Henclewood and Daiheng Ni. The Development of a Dynamic-Interactive-Vehicle Model for Modeling Traffic beyond the Microscopic Level. In *Pre-print CD-ROM, the 87th Transportation Research Board (TRB) Annual Meeting*, Washington, D.C., January 13-17, 2008.

[63] Dwayne Henclewood. The Development of a Dynamic-Interactive-Vehicle Model for Modeling Traffic beyond the Microscopic Level. Master's thesis, Department of Civil and Environmental Engineering, University of Massachusetts, Amherst, MA, September 2007.

[64] Daiheng Ni and Dwayne Henclewood. Simple Engine Models for VII-Enabled In-Vehicle Applications. *To appear in: IEEE Transactions on Vehicular Technology*, 57(5), 2008.

[65] Daiheng Ni and Qun Yu. A Neural Network for Handling Stability of Driver-Vehicle-Environment Closed-Loop System. *Journal of China Agricultural University (In Chinese)*, 1(2), 1996.

[66] Richard C. Tolman. *The Principles of Statistical Mechanics*. Dover Publications, 1980.

[67] Stewart Harris. *An Introduction to the Theory of the Boltzmann Equation*. Dover Books on Physics. Dover Publications, 2004.

[68] H.J. Payne. FREFLO: A Macroscopic Simulation Model for Freeway Traffic. *Transportation Research Record*, 722:68–77, 1979.

[69] C.F. Daganzo. A Finite Difference Approximation of the Kinematic Wave Model of Traffic Flow. *Transportation Research B*, 29(4):261–276, 1995.